Available online at www.sciencedirect.com
ScienceDirect
Journal of Computational Physics 227 (2008) 5492–5512
JOURNAL OF COMPUTATIONAL PHYSICS
www.elsevier.com/locate/jcp

Multi-symplectic integration of the Camassa–Holm equation

David Cohen *, Brynjulf Owren, Xavier Raynaud

Department of Mathematical Sciences, NTNU, NO-7491 Trondheim, Norway

Received 6 July 2007; received in revised form 22 January 2008; accepted 29 January 2008
Available online 9 February 2008

Abstract

The Camassa–Holm equation is rich in geometric structures, it is completely integrable, bi-Hamiltonian, and it represents geodesics for a certain metric in the group of diffeomorphism. Here two new multi-symplectic formulations for the Camassa–Holm equation are presented, and the associated local conservation laws are shown to correspond to certain well-known Hamiltonian functionals. The multi-symplectic discretisation of each formulation is exemplified by means of the Euler box scheme. Numerical experiments show that the schemes have good conservative properties, and one of them is designed to handle the conservative continuation of peakon–antipeakon collisions.

MSC: 35Q51; 35Q53; 37K05; 37K10; 37M15; 65M06; 65M99; 65P10

Keywords: Camassa–Holm equation; Multi-symplecticity; Euler box scheme; Peakon–antipeakon collisions; Conservation laws

1. Introduction

The aim of this paper is to study multi-symplectic algorithms for the numerical integration of the Camassa–Holm equation [6,7]

$$u_t - u_{xxt} + 3uu_x - 2u_xu_{xx} - uu_{xxx} = 0, \quad u|_{t=0} = u_0. \tag{1}$$

This partial differential equation has received considerable attention during the last decade. It is known to be rich in geometric structures and it possesses smooth as well as non-smooth traveling wave solutions. Thus, it seems natural to apply schemes which are known to retain at least some of these structures. We shall here be concerned in particular with the property of multi-symplecticy and investigate to which extent a simple numerical scheme with a similar property offers a worthwhile alternative to other known methods for this problem. In particular we are interested in understanding how the choice of a multi-symplectic formulation can be used as a guide for achieving the near-conservation of designated invariants.

* Corresponding author.
E-mail addresses: David.Cohen@math.ntnu.no (D. Cohen), Brynjulf.Owren@math.ntnu.no (B. Owren), Xavier.Raynaud@math.ntnu.no (X. Raynaud).

0021-9991/$ - see front matter © 2008 Elsevier Inc. All rights reserved.
doi:10.1016/j.jcp.2008.01.051

We begin by reviewing certain important properties of the Camassa–Holm equation. The equation models propagation of unidirectional gravitational waves in a shallow water approximation, with u representing the fluid velocity, see [6,28]. The Camassa–Holm equation also has applications in computational anatomy, see [27,36]. Eq. (1) can be rewritten in an equivalent manner as the following system

$$u_t + uu_x + P_x = 0, \tag{2a}$$

$$P - P_{xx} = u^2 + \frac{1}{2}u_x^2. \tag{2b}$$

The Camassa–Holm equation can be derived from a least action principle and it corresponds to the geodesic equation in the group of diffeomorphism with respect to a given right-invariant metric, see [15,16]. The equation has a bi-Hamiltonian structure [6,20,21] and is completely integrable [11]. It has infinitely many conserved quantities, see [6,19]. In particular, for smooth solutions the quantities

$$\int u\,\mathrm{d}x, \quad \int (u^2 + u_x^2)\,\mathrm{d}x, \quad \int (u^3 + uu_x^2)\,\mathrm{d}x \tag{3}$$

are all time independent (in this paper, we will not write the integration domain as the results hold for both solutions with periodic or vanishing at infinity boundary conditions).

The Camassa–Holm equation also possesses solutions of a soliton type, which, because of their shape, have been given the name of *peakons*. In the case of the real line, a single-peakon is given by

$$u(x,t) = c\,\mathrm{e}^{-|x-ct|},$$

thus, the traveling speed c is proportional to the height of the peak. In the periodic case with period a, the periodized version of this single-peakon is

$$u(x,t) = c\,\frac{\cosh(d(x-ct) - \frac{a}{2})}{\cosh(\frac{a}{2})},$$

where $d(x) = \min_{k\in\mathbb{Z}}|x - ka|$.

When the initial data u_0 is smooth enough, that is, $u_0 \in H^s(\mathbb{R})$ for $s > \frac{3}{2}$, the Cauchy problem for the Camassa–Holm equation is well-posed locally in time, see [14,33,38] for the non-periodic case. For initial data $u_0 \in H^1(\mathbb{R})$ which satisfies the condition that $u_0 - u_{0,xx}$ is a positive Radon measure, the solutions exist globally in time and are unique, see [17]. However, in the general case, solutions may blow-up and they do it in the following manner. Let T be the time where a smooth solution eventually loses its regularity, i.e., $\lim_{t\to T}\|u(\cdot,t)\|_{H^s} = \infty$ for all $s > 1$. Then,

$$\lim_{t\to T}\inf_{x\in\mathbb{R}} u_x(x,t) = -\infty.$$

There appears a point where the profile of u steepens gradually and ultimately the slope becomes vertical. In the context of water waves, this corresponds to the breaking of a wave [6,7,12,13]. After blow-up, the solution is no longer unique and the Camassa–Holm equation is indeed not well-posed globally in time. A good illustration of what may happen is given by the symmetric peakon–antipeakon case where two peakons which travel in opposite directions collide. Since the peakons have exactly opposite height, the solution at the time of collision, which we denote t^*, is identically zero, see Fig. 1.

After the time of collision, one can prolong the solution by letting the peakon and antipeakon "pass through" each other in a way which is consistent with the Camassa–Holm equation and such that the energy remains constant except at t^*. These solutions are called *conservative* as they preserve the energy for almost every time. It is clear that in order to obtain the conservative solutions out of the zero state which is reached at the time of collision, we need extra information. This information is provided by the energy density $(u^2 + u_x^2)\,\mathrm{d}x$. In the case of the antisymmetric peakon–antipeakon collision the energy density $(u^2 + u_x^2)\,\mathrm{d}x$ tends to a Dirac measure located at the point of collision and whose magnitude depends on the total energy of the solution, see [25] for detailed computations. A semigroup of global conservative collisions has been obtained in [2,24] via a change of coordinates. In [24], Lagrangian variables are used and the key point in the argument comes from the fact that the energy density satisfies the following transport equation

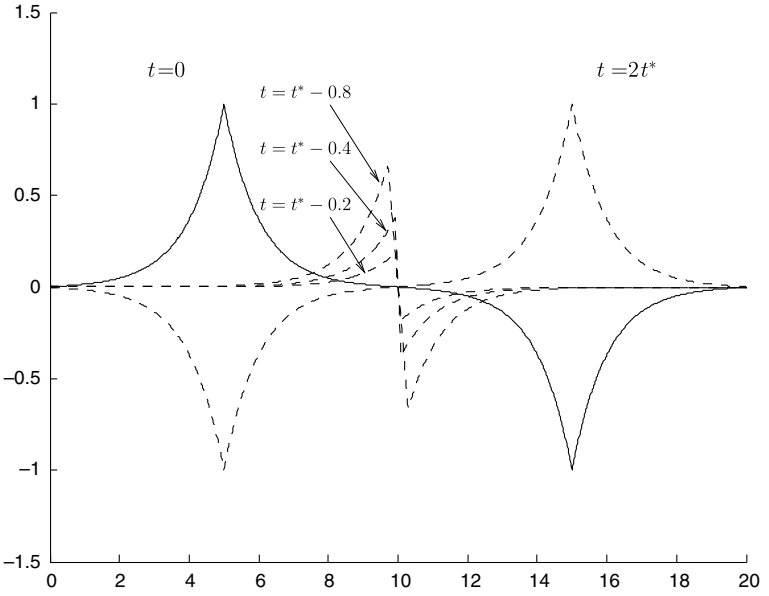

Fig. 1. Symmetric peakon–antipeakon collision.

$$(u^2+u_x^2)_t+(u(u^2+u_x^2))_x=(u^3-2Pu)_x, \tag{4}$$

where P is given by (2b). In this article we derive numerical methods which aim to resolve the conservative solutions, and to achieve this, we shall make explicit use of the evolution of the energy density. After denoting $u^2+u_x^2$ by α, we can see that (2) and (4) are equivalent to

$$u_t+uu_x+P_x=0, \tag{5a}$$

$$P-P_{xx}=\frac{1}{2}u^2+\frac{1}{2}\alpha, \tag{5b}$$

$$\alpha_t+(u\alpha)_x=(u^3-2Pu)_x. \tag{5c}$$

We now briefly review certain numerical schemes for the Camassa–Holm equation (1) found in the literature, but without intending to be exhaustive. Schemes using a pseudospectral space discretisation of the Camassa–Holm equation were derived in [7,30]. This last paper investigates numerically different aspects of periodic traveling waves and tries to understand the rate of convergence of the algorithm. An approach based on the multipeakons

$$u(x,t)=\sum_{i=1}^{n}p_i(t)\,\mathrm{e}^{-|x-q_i(t)|},$$

where p_i and q_i are solutions of the Hamiltonian system with Hamiltonian function $H(p,q)=\frac{1}{2}\sum_{i,j=1}^{n}p_ip_j\,\mathrm{e}^{-|q_i-q_j|}$, is examined in [8,9,23,26]. Amongst other things, the conditions for global existence and the convergence of the methods are studied in these articles. A convergence analysis of finite difference schemes was given in [10,22]. We mention that the schemes proposed in [10] and in [26] can also handle peakon–antipeakon collisions. In [1], a finite volume method is developed to simulate the dynamics of peakons. This scheme is adaptive, with high resolution and stable. Finally, a finite element method is derived in [40]. The scheme proposed in this paper is high order accurate and nonlinearly stable. Several numerical examples are also included in order to illustrate the behaviour and verify the properties of this method.

The rest of this paper is organised as follows: in Section 2 we review some of the general theory of multi-symplectic PDEs and their numerical discretisations, following the approach of Bridges and Reich [4]. In Section 3 we present two new multi-symplectic formulations of the Camassa–Holm equation, and discuss their

momentum and energy conservation laws. We consider discretisations using the multi-symplectic Euler box scheme and demonstrate their performance through numerical tests. Since the focus of our approach is mainly geometric, we shall be particularly interested in the conservative properties when we present the numerical experiments, and we make active use of the energy conservation in order to handle peakon–antipeakon collisions. However, for comparison with earlier work published in the literature, we also present some numerical results related to convergence on finite time.

2. Multi-symplectic PDEs and their multi-symplectic discretisation

2.1. Multi-symplectic partial differential equations

The schemes that we propose for the Camassa–Holm equation are based on multi-symplectic formulations of the partial differential equations (1) or (5). For the sake of completeness, we will review this concept in a general context, for more details, see e.g. [3,4,37].

A partial differential equation $F(u, u_t, u_x, u_{tx}, \ldots) = 0$ is said to be *multi-symplectic* if it can be written as a system of first order equations:

$$M z_t + K z_x = \nabla_z S(z), \tag{6}$$

with $z \in \mathbb{R}^d$ a vector of state variables, typically including the original variable u as one of its components. The matrices M and K are skew-symmetric $d \times d$-matrices, and S is a smooth scalar function depending on z. Eq. (6) is not necessarily unique and the dimension d of the state vector may differ from one expression to another. From the form of Eq. (6), we can see the multi-symplectic formulation of a partial differential equation as a natural generalisation of the symplectic formulation of the Hamiltonian system

$$J y_t = \nabla H(y),$$

where $J = \begin{pmatrix} 0 & I \\ -I & 0 \end{pmatrix}$. A key observation for the multi-symplectic formulation (6) is that M and K define symplectic structures on subspaces of $\mathbb{R}^d$,

$$\omega = \mathrm{d}z \wedge M \mathrm{d}z, \qquad \kappa = \mathrm{d}z \wedge K \mathrm{d}z.$$

Considering any pair of solutions to the variational equation associated with (6), we have, see [4], that the following *multi-symplectic conservation law* applies

$$\partial_t \omega + \partial_x \kappa = 0. \tag{7}$$

This is a *local* conservation law, and thus the multi-symplectic formulation of a partial differential equation may lead to numerical schemes which render well the local properties of the equation.

With the two skew-symmetric matrices M and K, one can also define the density functions

$$E(z) = S(z) - \frac{1}{2} z_x^{\mathrm{T}} K^{\mathrm{T}} z, \qquad F(z) = \frac{1}{2} z_t^{\mathrm{T}} K^{\mathrm{T}} z,$$
$$G(z) = S(z) - \frac{1}{2} z_t^{\mathrm{T}} M^{\mathrm{T}} z, \qquad I(z) = \frac{1}{2} z_x^{\mathrm{T}} M^{\mathrm{T}} z,$$

which immediately yield the *local conservation laws*

$$\partial_t E(z) + \partial_x F(z) = 0 \qquad \text{and} \qquad \partial_t I(z) + \partial_x G(z) = 0, \tag{8}$$

for any solution to (6). Thus, under the usual assumption on vanishing boundary terms for the functions $F(z)$ and $G(z)$ one obtains the globally conserved quantities of (*energy* and *momentum*)

$$\mathcal{E}(z) = \int E(z)\,\mathrm{d}x \qquad \text{and} \qquad \mathcal{I}(z) = \int I(z)\,\mathrm{d}x. \tag{9}$$

2.2. Multi-symplectic integrators

There are two standard ways to construct multi-symplectic integrators: one is to approximate the Lagrangian by a sum and take variations (see for example [35]), the other (see for example [3] or [4]) is to write the partial differential equation as a system of first order equations (6) and then to discretise it.

The main philosophy behind the use of symplectic integrators for Hamiltonian systems is that the schemes are designed to preserve the symplectic form of the equation at each time step. For multi-symplectic partial differential equations, the idea of Bridges and Reich [4] was to develop integrators which satisfy a discretised version of the multi-symplectic conservation law (7). For this purpose, they considered a direct discretisation of (6), replacing the derivatives with divided differences, and the continuous function $z(x,t)$ by a discrete version $z^{n,i} \approx z(x_n, t_i)$ on a uniform rectangular grid. We set $\Delta x = x_{n+1} - x_n, n \in \mathbb{Z},$ and $\Delta t = t_{i+1} - t_i$, $i \geqslant 0$.

Following their notation, we write

$$M\partial_t^{n,i} z^{n,i} + K\partial_x^{n,i} z^{n,i} = (\nabla_z S(z^{n,i}))^{n,i}, \tag{10}$$

where $\partial_t^{n,i}, \partial_x^{n,i},$ and $(\nabla_z S(z^{n,i}))^{n,i}$ are discretisations of the partial derivatives ∂_t, ∂_x and of the scalar function S, respectively. A natural way of inferring multi-symplecticity on the discrete level is to demand that for any pairs $(U^{n,i}, V^{n,i})$ of solutions to the corresponding variational equation of (10), one has

$$\partial_t^{n,i}\omega_{n,i} + \partial_x^{n,i}\kappa_{n,i} = 0,$$

where

$$\omega_{n,i}(U^{n,i}, V^{n,i}) = \langle MU^{n,i}, V^{n,i}\rangle, \qquad \kappa_{n,i}(U^{n,i}, V^{n,i}) = \langle KU^{n,i}, V^{n,i}\rangle.$$

Unfortunately, it is not generally true that the solutions of a multi-symplectic integrator fulfill the discrete versions of the local conservation laws for energy and momentum (8). However, as noted in [4] this holds when $S(z)$ is a quadratic function, but it is not the case for the multi-symplectic formulations of the Camassa–Holm equation which are presented here. We proceed by giving two well-known examples of multi-symplectic integrators, but first we introduce some notation for difference operators which will be used throughout the rest of this paper. For any variable $U = (U^{n,i})$ defined on a two-dimensional grid, we let

$$\delta_t^+ U^{n,i} = \frac{U^{n,i+1} - U^{n,i}}{\Delta t} \qquad \text{and} \qquad \delta_t^- U^{n,i} = \frac{U^{n,i} - U^{n,i-1}}{\Delta t},$$

and similarly for differences in space. Also, we shall need the centered differences $\delta_t = \frac{1}{2}(\delta_t^+ + \delta_t^-)$, and $\delta_x = \frac{1}{2}(\delta_x^+ + \delta_x^-)$.

2.2.1. The concatenated midpoint rule

This scheme, introduced by Preissman in 1960 and one of the most widely used in hydraulics, was proved to be multi-symplectic in [4]. The scheme also appears under the name of Preissman box scheme, or centered box scheme. It reads

$$M\delta_t^+\left(\frac{z^{n,i} + z^{n+1,i}}{2}\right) + K\delta_x^+\left(\frac{z^{n,i} + z^{n,i+1}}{2}\right) = \nabla_z S(z_c),$$

where

$$z_c = \frac{1}{4}(z^{n,i} + z^{n+1,i} + z^{n,i+1} + z^{n+1,i+1}).$$

2.2.2. The Euler box scheme

Following [37] one may obtain an integrator satisfying a discrete multi-symplectic conservation law by introducing a splitting of the two matrices M and K, setting $M = M_+ + M_-, K = K_+ + K_-$ where $M_+^{\mathrm{T}} = -M_-$ and $K_+^{\mathrm{T}} = -K_-$. The corresponding scheme reads

$$M_+\delta_t^+ z^{n,i} + M_-\delta_t^- z^{n,i} + K_+\delta_x^+ z^{n,i} + K_-\delta_x^- z^{n,i} = \nabla_z S(z^{n,i}). \tag{11}$$

Note that the scheme is only linearly implicit as opposed to the concatenated midpoint rule for which a system of nonlinear equations must be solved in each time step. The multi-symplecticity is interpreted in the sense that

$$\delta_t^+ \omega^{n,i} + \delta_x^+ \kappa^{n,i} = 0, \tag{12}$$

where $\omega^{n,i} = \mathrm{d}z^{n,i-1} \wedge M_+ \mathrm{d}z^{n,i}$ and $\kappa^{n,i} = \mathrm{d}z^{n-1,i} \wedge K_+ \mathrm{d}z^{n,i}$. An important observation is that the splitting of the matrices is not unique, and we shall see later that the choice of splitting may strongly affect the behaviour of the scheme. In general one can write, say $K_+ = \frac{1}{2}K + S$ and $K_- = \frac{1}{2}K - S$ where S is any symmetric matrix.

In the rest of the paper, we will consider only the Euler box scheme for the sake of simplicity, although in principle, any other multi-symplectic schemes could have been used.

3. Multi-symplectic integrators for the Camassa–Holm equation

In this section, we propose two multi-symplectic formulations for the Camassa–Holm equation. The first formulation is based on the partial differential equation (1) and has a state variable vector of dimension 5. The second formulation has eight components in the vector of state variables and it is based on (5). With this formulation the resulting multi-symplectic integrator is able to continue the conservative solution after a peakon–antipeakon collision.

3.1. First multi-symplectic formulation

Eq. (1) may be rewritten in the form

$$u_t - u_{xxt} + \left(\frac{3}{2}u^2 + \frac{1}{2}u_x^2\right)_x - (uu_x)_{xx} = 0. \tag{13}$$

Setting $z = [u, \phi, w, v, v]^{\mathrm{T}}$ we may now derive a multi-symplectic formulation (6) with the two skew-symmetric matrices

$$M = \begin{bmatrix} 0 & \frac{1}{2} & 0 & 0 & -\frac{1}{2} \\ -\frac{1}{2} & 0 & 0 & 0 & 0 \\ 0 & 0 & 0 & 0 & 0 \\ 0 & 0 & 0 & 0 & 0 \\ \frac{1}{2} & 0 & 0 & 0 & 0 \end{bmatrix}, \qquad K = \begin{bmatrix} 0 & 0 & 0 & -1 & 0 \\ 0 & 0 & 1 & 0 & 0 \\ 0 & -1 & 0 & 0 & 0 \\ 1 & 0 & 0 & 0 & 0 \\ 0 & 0 & 0 & 0 & 0 \end{bmatrix}.$$

The right-hand side of (6) is then given by the gradient of the scalar function

$$S(z) = -wu - u^3/2 - uv^2/2 + vv.$$

For convenience, we also write this system componentwise

$$\begin{aligned} &\frac{1}{2}\phi_t - \frac{1}{2}v_t - v_x = -w - \frac{3}{2}u^2 - \frac{1}{2}v^2, \\ &-\frac{1}{2}u_t + w_x = 0, \\ &\phi_x = u, \\ &-u_x = -v, \\ &-\frac{1}{2}u_t = uv - v. \end{aligned}$$

To the best of our knowledge, this multi-symplectic formulation of the Camassa–Holm equation is new. However, in the Lagrangian setting a formulation with 6×6 matrices M and K has been derived in [31] and a formulation with non-constant matrices can be found in [18].

For this choice of the skew-symmetric matrices M and K, the density functions defined in the introduction are explicitly given by

$$E(z) = S(z) + \frac{1}{2} z_x^{\mathrm{T}} K z = \frac{1}{4}(\phi_t u - u_{xt} u + u^3 + u_x u_t + u u_x^2 - u_t \phi),$$

$$F(z) = -\frac{1}{2} z_t^{\mathrm{T}} K z = \frac{1}{2}(u_t v - \phi_t w + \phi w_t - u v_t),$$

$$G(z) = S(z) + \frac{1}{2} z_t^{\mathrm{T}} M z = \frac{1}{2}\phi_t u - u_{xt} u - u^2 u_{xx} + u^3 - \frac{1}{2} u_x^2 + \frac{1}{2} u u_x^2 + \frac{1}{2} u_x u_t + \frac{1}{4}(u_t \phi - u_t v - \phi_t u + v_t u),$$

$$I(z) = -\frac{1}{2} z_x^{\mathrm{T}} M z = \frac{1}{4}(-u_x \phi + u_x v + u \phi_x - u v_x).$$

In deriving the corresponding global invariants (9), some care has to be taken with respect to boundary terms because $\phi(x,t)$ is not periodic (or vanishing at $\pm\infty$) even if $u(x,t)$ is. We integrate the second local conservation law $\partial_t I(z) + \partial_x G(z) = 0$ over the spatial domain and obtain (using the definitions of the additional variables)

$$\frac{1}{4}\frac{\mathrm{d}}{\mathrm{d}t}\int (-u_x \phi + u_x^2 + u^2 - u u_{xx})\,\mathrm{d}x + [G(z)] = 0, \tag{14}$$

where the square brackets denote the difference of the function evaluated at the upper and lower limit of the integral. The periodic (or vanishing at infinity) boundary conditions of u imply that $[u] = [u_x] = [u_{xx}] = \cdots = 0$ and $[\phi_t] = \int \phi_{xt}\,\mathrm{d}x = \int u_t\,\mathrm{d}x = \int (\frac{u^2}{2} + P)_x\,\mathrm{d}x = 0$. Hence, after two integrations by parts, it follows from (14) that

$$\frac{1}{2}\frac{\mathrm{d}}{\mathrm{d}t}\int (u^2 + u_x^2)\,\mathrm{d}x - \frac{1}{4}\frac{\mathrm{d}}{\mathrm{d}t}[u\phi] + \frac{1}{4}[u_t \phi] = 0,$$

and thus the momentum $\int (u^2 + u_x^2)\,\mathrm{d}x$ is a global conserved quantity.

Similarly, for the energy, we obtain

$$-2\frac{\mathrm{d}}{\mathrm{d}t}\int (u^3 + u_x^2 u)\,\mathrm{d}x + \frac{\mathrm{d}}{\mathrm{d}t}\left[\frac{1}{4}(\phi_t - 2\phi_{xxt} - \phi_{xx}^2 + 3\phi_x^2 - 2\phi_x \phi_{xxx})\phi\right] + \frac{1}{2}[\phi w_t] = 0.$$

By the usual assumption on boundary terms, the two expressions in square brackets cancel.

Finally, we remark that these two global conserved quantities are equivalent to the two Hamiltonians of the bi-Hamiltonian formulation of the Camassa–Holm equation given for instance in [6,34]:

$$\mathcal{H}_1 = \frac{1}{2}\int (u^2 + u_x^2)\,\mathrm{d}x, \tag{15}$$

$$\mathcal{H}_2 = \frac{1}{2}\int (u^3 + u u_x^2)\,\mathrm{d}x. \tag{16}$$

Considering now waves traveling from left to right, we have chosen the following splitting of M and K

$$M_+ = \begin{bmatrix} 0 & 0 & 0 & 0 & 0 \\ -\frac{1}{2} & 0 & 0 & 0 & 0 \\ 0 & 0 & 0 & 0 & 0 \\ 0 & 0 & 0 & 0 & 0 \\ \frac{1}{2} & 0 & 0 & 0 & 0 \end{bmatrix}, \quad \text{and} \quad K_+ = \begin{bmatrix} 0 & 0 & 0 & -1 & 0 \\ 0 & 0 & 1 & 0 & 0 \\ 0 & 0 & 0 & 0 & 0 \\ 0 & 0 & 0 & 0 & 0 \\ 0 & 0 & 0 & 0 & 0 \end{bmatrix}.$$

With this particular choice, the Euler box scheme (11) reads

$$\frac{1}{2}\delta_t^- \phi^{n,i} - \frac{1}{2}\delta_t^- v^{n,i} - \delta_x^+ v^{n,i} = -w^{n,i} - \frac{3}{2}(u^{n,i})^2 - \frac{1}{2}(v^{n,i})^2,$$

$$-\frac{1}{2}\delta_t^+ u^{n,i} + \delta_x^+ w^{n,i} = 0,$$

$$-\delta_x^- \phi^{n,i} = -u^{n,i},$$

$$\delta_x^- u^{n,i} = v^{n,i},$$
$$\frac{1}{2}\delta_t^+ u^{n,i} = -u^{n,i}v^{n,i} + v^{n,i}.$$

There is a potential difficulty in the computation of the starting values $z^{n,0}$ and in the recurrence for $\phi^{n,i}$. But fortunately, like in [39] for the KdV equation, one can eliminate all the additional variables ϕ, w, v, v and express the Euler box scheme only in terms of the variable u. This gives us the following multi-symplectic integrator, which can be compared to the form (13) of the Camassa–Holm equation

$$\frac{1}{2}(\delta_t^+ + S_x\delta_t^-)u^{n,i} - \frac{1}{2}\delta_x^+(\delta_x^-\delta_t^- + \delta_x^+\delta_t^+)u^{n,i} + \delta_x^+\left(\frac{3}{2}(u^{n,i})^2 + \frac{1}{2}(\delta_x^- u^{n,i})^2 - \delta_x^+(u^{n,i}\delta_x^- u^{n,i})\right) = 0, \tag{17}$$

where we have introduced the right shift operator $S_x u^{n,i} = u^{n+1,i}$.

In the case where the wave travels in the opposite direction, one must use a different splitting of the skew-symmetric matrix K, for example

$$K_+ = \begin{bmatrix} 0 & 0 & 0 & 0 & 0 \\ 0 & 0 & 0 & 0 & 0 \\ 0 & -1 & 0 & 0 & 0 \\ 1 & 0 & 0 & 0 & 0 \\ 0 & 0 & 0 & 0 & 0 \end{bmatrix}.$$

The resulting numerical scheme and its behaviour is very similar to the first case, and we therefore omit any further discussion of it. In the case of waves traveling in both directions simultaneously, it is possible to make a compromise between the two above choices, and set $K_+ = \frac{1}{2}K$ and $M_+ = \frac{1}{2}M$. The resulting scheme is given below, expressed only in terms of the variable u and using the centered divided differences δ_t, δ_x:

$$\delta_t u^{n,i} - \delta_x^2\delta_t u^{n,i} + \delta_x\left(\frac{3}{2}(u^{n,i})^2 + \frac{1}{2}(\delta_x u^{n,i})^2\right) - \delta_x^2(u^{n,i}\delta_x u^{n,i}) = 0. \tag{18}$$

In Fig. 2, we plot the deviation of the invariants (3) from their initial values along the numerical solution obtained by the Euler box scheme, using the schemes (17) and (18), respectively. We have used the following smooth initial data (see [1])

$$u_0(x) = u(x,0) = 0.2 + 0.1\cos(2x), \quad \text{for } x \in [-\pi, \pi],$$

and grid parameters $\Delta x = 0.0042$ and $\Delta t = 0.004$ over the time interval [0, 5]. It is interesting to observe how sensitive the conservation properties are to the choice of the splitting of the matrix K.

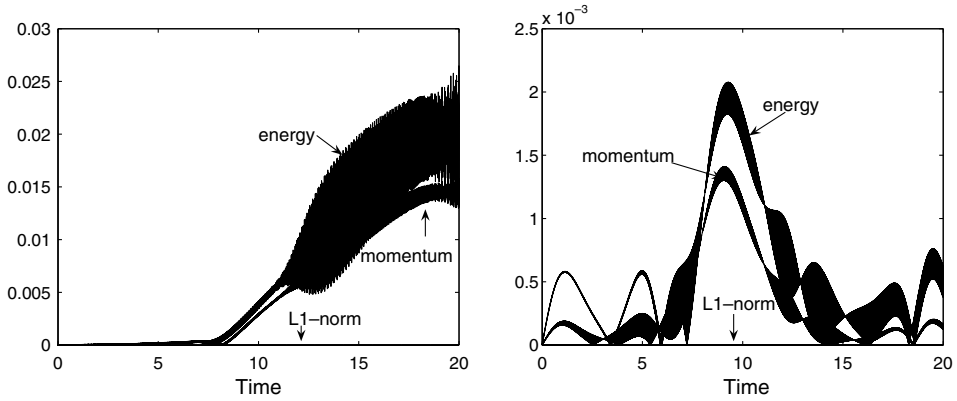

Fig. 2. Conservation properties of scheme (17) (left) and the scheme based on centered splitting (18) (right) for smooth initial data.

The Camassa–Holm equation admits a whole family of traveling waves of the type

$$u(x,t) = f(x - ct),$$

where f is a function of one variable and c is the velocity of the wave, see [32]. It can be checked that smooth traveling waves have to fulfill the relation

$$\frac{\mathrm{d}^2 f}{\mathrm{d}x^2} = f - \frac{\alpha}{(f-c)^2}, \tag{19}$$

for some constant α. To obtain a periodic smooth traveling wave the constant α cannot be taken arbitrarily, as pointed out by Kalisch [29]. By choosing $c = \alpha = 3$ and solving (19) for $f(0) = 1$ and $f\prime(0) = 0$, we obtain a periodic smooth traveling wave with period $a = 6.469546942524$, see Fig. 3.

We consider the convergence of the scheme (18) for a smooth traveling wave with initial data as in Fig. 3. The Courant number $p = \frac{c\Delta t}{\Delta x}$ is fixed to the value $p = 0.9$. We vary the space step x and set the time step to $\Delta t = p\Delta x/c$. Table 1 displays the L^1-error and an order estimate at time $T = 12$ for various space step Δx. For this smooth solution, order 2 can be observed.

In the following numerical experiment, we study the error for the peakon solution (see [40]) given by

$$u_0(x) = \begin{cases} \frac{c}{\cosh(a/2)} \cosh(x - x_0) & \text{if } |\, x - x_0 \,| \leqslant a/2, \\ \frac{c}{\cosh(a/2)} \cosh(a - (x - x_0)) & \text{if } |\, x - x_0 \,| > a/2, \end{cases} \tag{20}$$

where $x_0 = -5$, $c = 1$ and the period $a = 30$. Fig. 4 shows snapshots, for the time $t = 0, 3$ and 5, of the exact solution (solid line) and the numerical solution (dashed line) computed with a time step $\Delta t = 0.0002$ and a space step $\Delta x = 0.04$ for method (18). Note that even for this relatively small space step, a small oscillatory tail at one end of the peak appears in the numerical solution. This phenomenon was also observed in [30].

We next consider the rate of convergence for the problem (20) using again the scheme (18), the Courant number $p = \frac{c\Delta t}{\Delta x}$ is fixed to the value $p = 0.9$. We vary the space step Δx and set the time step to $\Delta t = p\Delta x/c$. One can see from Fig. 5 that the order of convergence is one for this non-smooth solution.

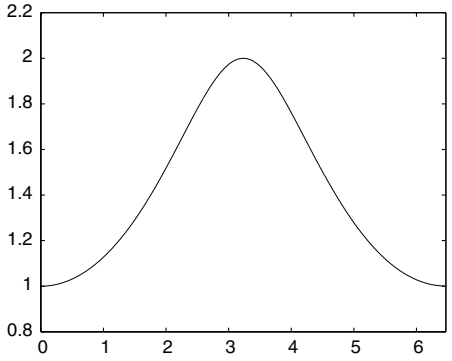

Fig. 3. Smooth periodic traveling wave.

Table 1
Convergence rate for the smooth traveling wave (19)

Δx	L^1-error	Order estimate
2.5272e−02	2.5168e−03	–
1.2636e−02	6.2909e−04	2.0003
6.3179e−03	1.5724e−04	2.0003
3.1590e−03	3.9311e−05	1.9999
2.1060e−03	1.7473e−05	1.9998
1.5795e−03	9.8285e−06	2.0000
1.2636e−03	6.2903e−06	2.0000
1.0783e−03	4.5805e−06	1.9999
8.0869e−04	2.5767e−06	1.9998

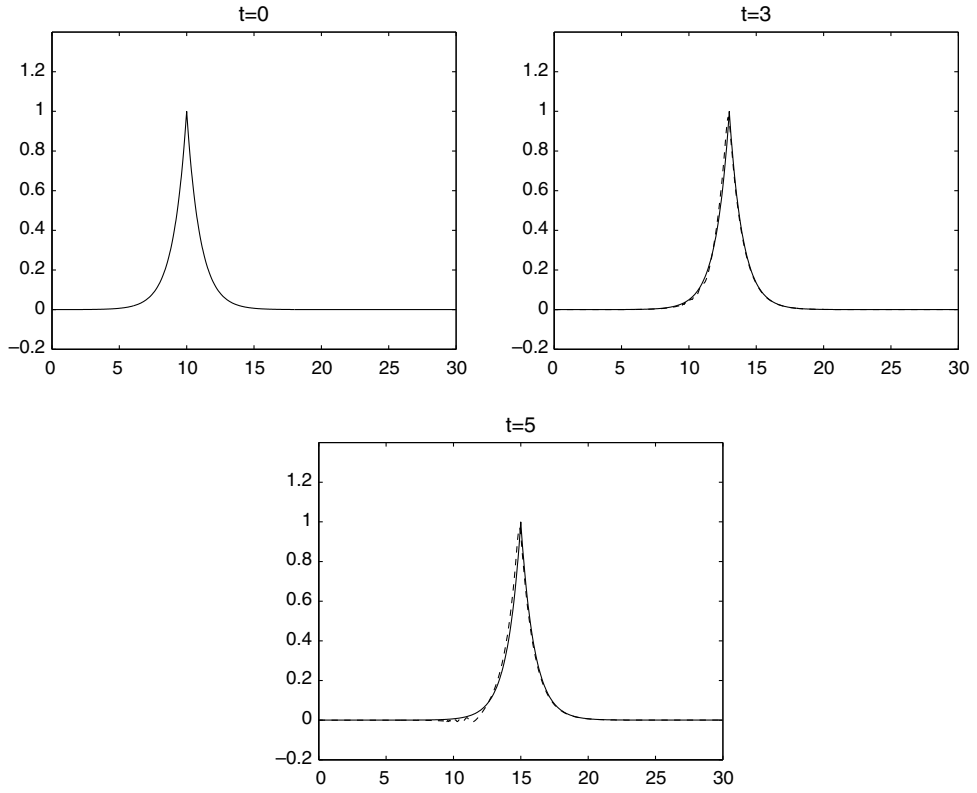

Fig. 4. Snapshots of the peakon solution and the numerical solution given by (18).

3.2. Second multi-symplectic formulation

As we said in the beginning of this section, the first formulation does not handle peakon–antipeakon collisions. To remedy to this problem, as explained in the introduction, in addition we will consider the evolution of the energy density and replace Eq. (2) by (5). However, we first have to prove that the two formulations are indeed equivalent. When the solutions are smooth, Eq. (2) implies (5); the computation which is very similar to the one that follows can also be found in [24]. We want to establish the implication in the opposite direction. We consider a solution (u, α) of (5) with initial data (u_0, α_0) satisfying $\alpha_0(x) = u_0^2(x) + u_{0x}^2(x)$ and we want to prove that u is solution of (2). It will be the case if we can prove that for any time $t > 0$, $\alpha(x,t)$ remains equal to $u^2(x,t) + u_x^2(x,t)$ as the Eqs. (5a) and (5b) become then identical to Eq. (2). After differentiating (5a) and using (5b), we obtain

$$u_{tx} + u_x^2 + uu_{xx} = \frac{1}{2}u^2 + \frac{1}{2}\alpha - P.$$

We multiply both sides by $2u_x$ and after some manipulations we obtain

$$(u_x^2)_t + u(u_x^2)_x = u^2u_x + \alpha u_x - 2Pu_x - 2u_x^3. \tag{21}$$

After multiplying (5a) by $2u$, we obtain

$$(u^2)_t + u(u^2)_x + 2P_x u = 0. \tag{22}$$

Let us denote the difference $\alpha - (u^2 + u_x^2)$ by w. Subtracting (21) and (22) to (5c), we obtain after some calculations that

$$w_t + uw_x = -2u_x w. \tag{23}$$

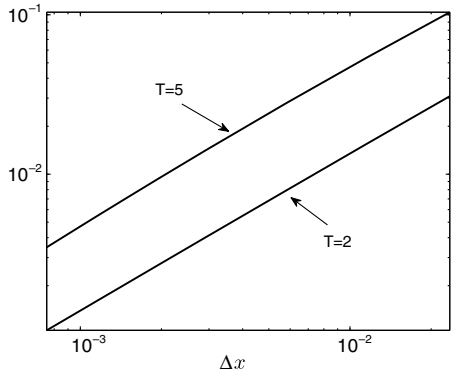

Fig. 5. L^1-error of the centered scheme at $T = 2$ and $T = 5$ applied to the single-peakon problem with initial data (20) where $x_0 = 0, a = 6, c = 1$.

We have $w(x,0) = \alpha_0(x) - u_0^2(x) + u_{0,x}^2(x) = 0$. We claim that $w(x,t) = 0$ for all $t > 0$ and therefore the systems (2) and (5) are equivalent. Recalling the assumption that u is smooth, we can define the characteristics $y(\xi,t)$ as $y_t(\xi,t) = u(y(\xi,t),t)$ with $y(\xi,0) = \xi$ and the mapping $\xi \to y(\xi,t)$ is a bijection for all time t. We consider the quantity $W(\xi,t) = w(y(\xi,t),t)$. Since $W_t = w_t(y,t) + u(y,t)w_x(y,t)$, it follows from (23) that

$$W_t(\xi,t) = -2u_x(y,t)W(\xi,t).$$

Since we assume that u is smooth, we have $C = \sup_{(x,t)\in\mathbb{R}\times[0,T]} \mid u_x(x,t) \mid < \infty$ and

$$\mid W_t \mid \leqslant C \mid W \mid .$$

As $W(\xi,0) = w(\xi,0) = 0$, Gronwall's Lemma gives us that $W(\xi,t) = 0$ for all t and ξ and therefore $w(x,t) = 0$ for all t and x, as claimed. Of course, the condition that u is smooth is a strong limitation since it does not cover the collision case, which was the case which motivated the introduction of the system (5). However, one must keep in mind that the uniqueness of the conservative solutions in [2,24] is only obtained in the new sets of variables where they are defined and that there is no uniqueness result – to the knowledge of the authors – for the equation expressed in the original variable u, even if it would be reasonable to conjecture that the solution of

$$u_t + uu_x + P_x = 0,$$
$$P - P_{xx} = u^2 + \frac{1}{2}u_x^2,$$
$$(u^2 + u_x^2)_t + (u(u^2 + u_x^2))_x = (u^3 - 2Pu)_x$$

is unique and given by the conservative solutions. But this is an open problem and from this perspective, the fact that the numerical solutions of (5) we obtain below coincide with the conservative solutions of the problem reinforces this conjecture.

Let us introduce a multi-symplectic formulation based on (5).

Let $z = [u, \beta, w, \alpha, \phi, \gamma, P, r]$,

$$M = \begin{bmatrix} 0 & -\frac{1}{2} & 0 & 0 & 0 & 0 & 0 & 0 \\ \frac{1}{2} & 0 & 0 & 0 & 0 & 0 & 0 & 0 \\ 0 & 0 & 0 & 0 & 0 & 0 & 0 & 0 \\ 0 & 0 & 0 & 0 & -\frac{1}{2} & 0 & 0 & 0 \\ 0 & 0 & 0 & \frac{1}{2} & 0 & 0 & 0 & 0 \\ 0 & 0 & 0 & 0 & 0 & 0 & 0 & 0 \\ 0 & 0 & 0 & 0 & 0 & 0 & 0 & 0 \\ 0 & 0 & 0 & 0 & 0 & 0 & 0 & 0 \end{bmatrix}, \qquad K = \begin{bmatrix} 0 & 0 & 0 & 0 & 0 & 0 & 0 & 0 \\ 0 & 0 & 1 & 0 & 0 & 0 & 1 & 0 \\ 0 & -1 & 0 & 0 & 0 & 0 & 0 & 0 \\ 0 & 0 & 0 & 0 & 0 & 0 & 0 & 0 \\ 0 & 0 & 0 & 0 & 0 & 1 & 0 & 0 \\ 0 & 0 & 0 & 0 & -1 & 0 & 0 & 0 \\ 0 & -1 & 0 & 0 & 0 & 0 & 0 & -2 \\ 0 & 0 & 0 & 0 & 0 & 0 & 2 & 0 \end{bmatrix}$$

and

$$S = -\gamma u + \frac{u^2\alpha}{2} - \frac{u^4}{4} + Pu^2 - \alpha w - P^2 + r^2.$$

The multi-symplectic formulation (6) is equivalent to the following system

$$\begin{aligned}
&-\frac{1}{2}\beta_t = -\gamma + u\alpha - u^3 + 2Pu, \quad \frac{1}{2}u_t + w_x + P_x = 0,\\
&-\beta_x = -\alpha, \qquad -\frac{1}{2}\phi_t = -w + \frac{u^2}{2},\\
&\frac{1}{2}\alpha_t + \gamma_x = 0, \qquad -\phi_x = -u,\\
&-\beta_x - 2r_x = -2P + u^2, \qquad 2P_x = 2r.
\end{aligned} \tag{24}$$

We now find the energy and momentum corresponding to this multi-symplectic formulation. As for the first formulation, the density functions are given by

$$\begin{aligned}
E(z) &= -\gamma\phi_x + \frac{u^2\alpha}{2} - \frac{u^4}{4} + Pu^2 - \alpha w - P^2 + P_x^2 + \frac{1}{2}\beta_x(w+P) - \frac{1}{2}w_x\beta + \frac{1}{2}\phi_x\gamma - \frac{1}{2}\gamma_x\phi - \frac{1}{2}P_x(2P_x+\beta)\\
&\quad + P_{xx}P,\\
F(z) &= -\frac{1}{2}\beta_t(w+P) + \frac{1}{2}w_t\beta - \frac{1}{2}\phi_t\gamma + \frac{1}{2}\gamma_t\phi + \frac{1}{2}P_t(2P_x+\beta) - P_{xt}P,\\
G(z) &= -\gamma\phi_x + \frac{u^2\alpha}{2} - \frac{u^4}{4} + Pu^2 - \alpha w - P^2 + P_x^2 - \frac{1}{4}(u_t\beta - \beta_t u + \alpha_t\phi - \phi_t\alpha),\\
I(z) &= \frac{1}{4}(u_x\beta - \beta_x u + \alpha_x\phi - \phi_x\alpha).
\end{aligned}$$

The first conservation law $\partial_t E(z) + \partial_x F(z) = 0$ yields

$$\begin{aligned}
&\frac{\mathrm{d}}{\mathrm{d}t}\int\left(-\gamma\phi_x + \frac{1}{2}\phi_x\gamma - \frac{1}{2}\gamma_x\phi - \beta_x w + \frac{1}{2}\beta_x w - \frac{1}{2}w_x\beta - \frac{1}{2}P_x\beta + \frac{u^2\alpha}{2} - \frac{u^4}{4}\right.\\
&\quad \left. + Pu^2 - P^2 + P_x^2 + \frac{1}{2}\alpha P - P_x^2 + P_{xx}P\right)\mathrm{d}x\\
&\quad + \frac{1}{2}[w_t\beta + \gamma_t\phi + P_t\beta] = 0.
\end{aligned}$$

Integrating the terms $-\frac{1}{2}\gamma_x\phi, -\frac{1}{2}w_x\beta$ and $-\frac{1}{2}P_x\beta$ by parts, and using the periodicity (or vanishing at infinity) of the functions u, P, w, ϕ_t, β_t, we obtain that

$$\frac{\mathrm{d}}{\mathrm{d}t}\int\left(\left(u^2 + \frac{u_x^2}{2}\right)P + \frac{u^2}{4}(u^2 + 2u_x^2)\right)\mathrm{d}x = 0.$$

The second local conservation law $\partial_t I(z) + \partial_x G(z) = 0$ leads to

$$\frac{1}{4}\frac{\mathrm{d}}{\mathrm{d}t}\int(u_x\beta - \alpha u + \alpha_x\phi - \alpha u)\,\mathrm{d}x + [G(z)] = 0.$$

And two integrations by parts give the global conservation of $\int(u^3 + u_x^2 u)\,\mathrm{d}x$. We thus obtain the following two global conserved quantities

$$\mathcal{H}_2 = \int(u^3 + u_x^2 u)\,\mathrm{d}x, \tag{25}$$

$$\mathcal{H}_3 = \int\left(\left(u^2 + \frac{u_x^2}{2}\right)P + \frac{u^2}{4}(u^2 + 2u_x^2)\right)\mathrm{d}x, \tag{26}$$

which correspond to the third and fourth Hamiltonian in the series of constant of motion of the Camassa–Holm equation.

Considering again (24), we see that after eliminating the intermediate variables β, w, ϕ, γ and r, the system (5) is recovered. The computation is identical to the discrete case which is treated below. We use symmetric splittings of M and K and take $M_+ = M_- = \frac{1}{2}M$ and $K_+ = K_- = \frac{1}{2}K$. The Euler box scheme is then obtained from (24) by replacing the exact derivatives, ∂_t and ∂_x, by their discrete symmetric counterparts, δ_t and δ_x. We have

$$-\frac{1}{2}\delta_t\beta^{n,i} = -\gamma^{n,i} + u^{n,i}\alpha^{n,i} - (u^{n,i})^3 + 2P^{n,i}u^{n,i}, \quad \frac{1}{2}\delta_t u^{n,i} + \delta_x w^{n,i} + \delta_x P^{n,i} = 0, \tag{27a}$$

$$-\delta_x\beta^{n,i} = -\alpha^{n,i}, \qquad -\frac{1}{2}\delta_t\phi^{n,i} = -w^{n,i} + \frac{(u^{n,i})^2}{2}, \tag{27b}$$

$$-\delta_x\phi^{n,i} = -u^{n,i}, \quad \frac{1}{2}\delta_t\alpha^{n,i} + \delta_x\gamma^{n,i} = 0, \tag{27c}$$

$$-\delta_x\beta^{n,i} - 2\delta_x r^{n,i} = -2P^{n,i} + (u^{n,i})^2, \quad 2\delta_x P^{n,i} = 2r^{n,i}. \tag{27d}$$

As for the first multi-symplectic formulation, we eliminate the intermediate variables. Applying δ_x to both sides of the first equation in (27a), we obtain

$$-\frac{1}{2}\delta_x\delta_t\beta^{n,i} = -\delta_x\gamma^{n,i} + \delta_x(u^{n,i}\alpha^{n,i} - (u^{n,i})^3 + 2P^{n,i}u^{n,i}). \tag{28}$$

The operators δ_t and δ_x commute. Plugging $\delta_x\beta^{n,i} = \alpha^{n,i}$ and $\delta_x\gamma^{n,i} = -\frac{1}{2}\delta_t\alpha^{n,i}$ into (28) we obtain

$$\delta_t\alpha^{n,i} + \delta_x(u^{n,i}\alpha^{n,i}) = \delta_x((u^{n,i})^3 - 2P^{n,i}u^{n,i}), \tag{29}$$

which corresponds to the discretised version of (5c). Combining the first equation in (27b) and the two in (27d), we obtain

$$P^{n,i} - \delta_x\delta_x P^{n,i} = \frac{1}{2}(u^{n,i})^2 + \frac{1}{2}\alpha^{n,i}, \tag{30}$$

which corresponds to the discretised version of (5b). After applying δ_x to the second equation in (27b), we obtain

$$\delta_x w^{n,i} = \frac{1}{2}\delta_t\delta_x\phi^{n,i} + \delta_x\left(\frac{(u^{n,i})^2}{2}\right).$$

Plugging this into the second equation in (27a), since $\delta_x\phi^{n,i} = u^{n,i}$ from the first equation in (27c), we finally get

$$\delta_t u^{n,i} + \delta_x\left(\frac{(u^{n,i})^2}{2}\right) + \delta_x P^{n,i} = 0, \tag{31}$$

which is the discretised version of (5a). Gathering (31), (30) and (29), we obtain the following numerical scheme

$$\delta_t u^{n,i} + \delta_x\left(\frac{(u^{n,i})^2}{2}\right) + \delta_x P^{n,i} = 0, \tag{32a}$$

$$P^{n,i} - \delta_x\delta_x P^{n,i} = \frac{1}{2}(u^{n,i})^2 + \frac{1}{2}\alpha^{n,i}, \tag{32b}$$

$$\delta_t\alpha^{n,i} + \delta_x(u^{n,i}\alpha^{n,i}) = \delta_x((u^{n,i})^3 - 2P^{n,i}u^{n,i}). \tag{32c}$$

The numerical scheme (32) is the multi-symplectic Euler box scheme derived from the multi-symplectic formulation (6) and therefore it enjoys the conservation law (12). We also note that the scheme can be derived directly from (5) by taking the symmetric discretisation of the derivatives - both with respect to time and space – which appear in the system.

We consider the rate of convergence for the smooth traveling wave (19) using the scheme (32), the Courant number $p = \frac{c\Delta t}{\Delta x}$ is fixed to the value $p = 0.9$. We vary the space step Δx and set the time step to $\Delta t = p\Delta x/c$. Table 2 displays the L^1-error and an order estimate at time $T = 12$. This table can be compared to Table 1.

We next consider the convergence of the scheme (32) for the single-peakon problem with initial data (20) using $x_0 = 0, a = 6,$ and $c = 1$. Once again, the Courant number $p = c\Delta t/\Delta x$ is fixed to the value 0.9 and we vary Δx. A plot of the error at time $T = 2$ and $T = 5$ can be found in Fig. 6.

We want to study the behaviour of the numerical scheme when dealing with a collision. First we derive a reference solution for the antisymmetric peakon collision. We adapt the formulae derived in [25] to the periodic case. Let a denote the period. We consider the antisymmetric case and the positions of the peaks are given by

$$y_{2i}(t) = -y(t) + ia \quad \text{and} \quad y_{2i+1}(t) = y(t) + ia \tag{33}$$

while their height are given by

$$u_{2i}(t) = -u(t) \quad \text{and} \quad u_{2i+1}(t) = u(t) \tag{34}$$

for $i = 0, \pm 1, \pm 2, \ldots$. We denote the energy contained between the ith and $i + 1$th peak by $\delta H_i(t)$, that is, when the peaks do not coincide,

$$\delta H_i(t) = \int_{y_i}^{y_{i+1}} (u^2(x,t) + u_x^2(x,t))\,\mathrm{d}x. \tag{35}$$

In (35), $u(x,t)$ denotes the solution of (1) and not the height of the peak given in (34). Between two peaks, the function $u(x,t)$ is given as a linear combination of e^{-x} and e^{x} and therefore the integral in (35) can be computed. We obtain

Table 2
Convergence rate for the smooth traveling wave (19) for the scheme (32)

Δx	L^1-error	Order estimate
2.5272e−02	2.6017e−03	–
1.2636e−02	6.5045e−04	1.9999
6.3179e−03	1.6256e−04	2.0004
3.1590e−03	4.0644e−05	1.9999
2.1060e−03	1.8066e−05	1.9998
1.5795e−03	1.0162e−05	2.0001
1.2636e−03	6.5036e−06	1.9999
1.0783e−03	4.7358e−06	2.0000
8.0869e−04	2.6640e−06	1.9998

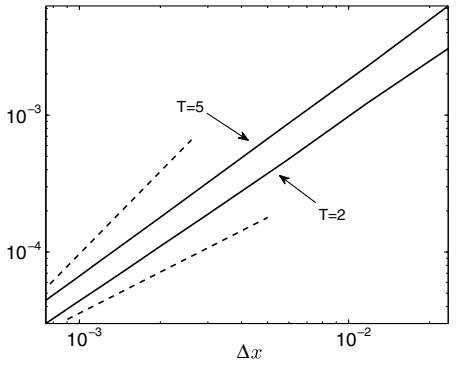

Fig. 6. L^1-error of the centered scheme at $T = 2$ and $T = 5$ applied to the single-peakon problem with initial data (20) using $x_0 = 0, a = 6,$ and $c = 1$. The dashed lines have slopes 1 and 2.

$$\delta H_i(t) = \frac{(u_i^2 + u_{i+1}^2)\cosh(y_{i+1} - y_i) - 2u_i u_{i+1}}{\sinh(y_{i+1} - y_i)}.$$

Note that when there is a collision, $y_{i+1} = y_i$, but this is a property of the quantity δH_i that it remains well-defined for all time. Note also that, at collision time, we have $\delta H_i > 0$ and not $\delta H_i = 0$ as (35) could indicate. In [25], the variable δH_i is considered as an independent variable and the equations that governs $(y_i, U_i, \delta H_i)$ are given by

$$\frac{\mathrm{d}}{\mathrm{d}t} y_i = u_i, \tag{36a}$$

$$\frac{\mathrm{d}}{\mathrm{d}t} u_i = -Q_i, \tag{36b}$$

$$\frac{\mathrm{d}}{\mathrm{d}t} \delta H_i = u_{i+1}^3 - u_i^3 - 2P_{i+1}u_{i+1} + 2P_i u_i, \tag{36c}$$

where

$$P_i = \sum_{j=-\infty}^{\infty} P_{i,j}, \text{ and } Q_i = -\sum_{j=-\infty}^{\infty} \kappa_{ij} P_{i,j}, \tag{37}$$

with

$$P_{i,j} = \frac{\exp(-\kappa_{ij} y_i)\exp(\kappa_{ij}\frac{y_j + y_{j+1}}{2})}{8\cosh(\frac{y_{j+1} - y_j}{2})}\left(2\delta H_j \cosh^2\left(\frac{y_{j+1} - y_j}{2}\right) + 2\kappa_{ij}(u_{j+1}^2 - u_j^2)\sinh^2\left(\frac{y_{j+1} - y_j}{2}\right) + (u_{j+1} + u_j)^2 \tanh\left(\frac{y_{j+1} - y_j}{2}\right)\right), \tag{38}$$

and

$$\kappa_{ij} = \begin{cases} -1 & \text{if } j \geqslant i \\ 1 & \text{otherwise.} \end{cases}$$

Due to the periodicity of the solution, δH_{2i} does not depend on i and we set $h = \delta H_{2i}$. We denote by E the energy over one period, that is, for times where *no* collision occurs,

$$E = \int_0^a (u^2(x,t) + u_x^2(x,t))\,\mathrm{d}x. \tag{39}$$

The quantity E is conserved and the energy contained between the $2i+1$th and $2i+2$th peaks is given by $\delta H_{2i+1} = E - h$. Using (33) and (34) we obtain from (38) and (37), after some calculation, that

$$Q_{2i} = -Q_{2i+1} = -E\frac{\cosh(\frac{a}{2} - y)\sinh(y)}{4\sinh(\frac{a}{2})} + \frac{h}{4} \tag{40}$$

and

$$P_i = E\frac{\cosh(\frac{a}{2} - y)\cosh(y)}{4\sinh(\frac{a}{2})}.$$

Then, (36) yields

$$y_t = u, \tag{41a}$$

$$u_t = -E\frac{\cosh(\frac{a}{2} - y)\sinh(y)}{4\sinh(\frac{a}{2})} + \frac{h}{4}, \tag{41b}$$

$$h_t = 2\left(u^3 - Eu\frac{\cosh(\frac{a}{2} - y)\cosh(y)}{2\sinh(\frac{a}{2})}\right). \tag{41c}$$

For the times when there is no collision, that is, when y is different from 0 or $\frac{a}{2}$, it is possible to compute explicitly the energy h and E from (39) and (35). We obtain

$$E = 2u^2 \frac{\sinh(\frac{a}{2})}{\sinh(y)\sinh(\frac{a}{2}-y)}, \tag{42}$$

and

$$h = 2u^2 \frac{\cosh(y)}{\sinh(y)}. \tag{43}$$

These expressions are not well-defined when $y = 0$ or $y = \frac{a}{2}$ but, after plugging (43) into (42), we get

$$h = E \frac{\sinh(\frac{a}{2}-y)\cosh(y)}{\sinh(\frac{a}{2})}, \tag{44}$$

which is well-defined even when collisions occur. Thus, we obtain an expression for h as a function only of y. In this simple case of an antisymmetric peakon–antipeakon collision, we did not integrate directly (36c), we rather used the fact that for almost every time, the density energy is given by $u^2 + u_x^2 \mathrm{d}x$ and therefore (35) and (39) hold. Of course, it is possible to derive (42) and (44) from the governing equations (41). To do that, one can introduce the quantities

$$w_1 = E\sinh\left(\frac{a}{2}-y\right)\cosh(y) - h\sinh\left(\frac{a}{2}\right)$$

and

$$w_2 = E\sinh(y)\sinh\left(\frac{a}{2}-y\right) - 2u^2\sinh\left(\frac{a}{2}\right).$$

From (41), after some computations, we obtain that

$$w_1' = uw_2,$$
$$w_2' = uw_1.$$

Hence, if (42) and (44) hold at time 0, that is $w_1(0) = w_2(0) = 0$, then, by Gronwall's Lemma, $w_1(t) = w_2(t) = 0$ for all t, that is, (42) and (44) hold for all time.

Finally, after plugging (44) into (40), Eqs. (36a) and (36b) yield

$$y_{tt} = \frac{E\sinh(\frac{a}{2}-2y)}{4\sinh(\frac{a}{2})}. \tag{45}$$

We outline here the computation of the trajectory of the peakons. For the sake of simplicity, we set the initial data to $y(0) = y_t(0) = 0$, that is, the peakons collide at time $t = 0$. We multiply (45) by y_t and after one integration get

$$\frac{1}{2}y_t^2 = \frac{E}{8\sinh(\frac{a}{2})}\left(\cosh\left(\frac{a}{2}\right) - \cosh\left(\frac{a}{2}-2y\right)\right), \tag{46}$$

where we have used the initial condition $y_t(0) = 0$. Making the change of variable $z = y - \frac{a}{4}$ in (46), we get

$$z_t^2 = \frac{E}{4\sinh\left(\frac{a}{2}\right)}\left(\cosh\left(\frac{a}{2}\right) - \cosh(2z)\right).$$

After simplifications, this leads to

$$\frac{z_t}{\sqrt{(1-k'^2\cosh^2(z))}} = \left(\frac{E\coth(\frac{a}{4})}{4}\right)^{\frac{1}{2}}, \tag{47}$$

where $k' = \frac{1}{\cosh(\frac{a}{4})}$. We set $k^2 = 1 - k'^2$ so that $k = \tanh(\frac{a}{4})$ and denote $\widetilde{\alpha} = (\frac{E\coth(\frac{a}{4})}{4})^{\frac{1}{2}}$. The expression on the left-hand side of (47) can be integrated with the help of Jacobi elliptic functions with *modulus* k, see e.g. [5], and we get

$$\cosh(z) = \mathrm{nd}(\widetilde{\alpha}t + A), \tag{48}$$

where A is a constant to be determined by the boundary condition. The constant A turns out to be equal to the *complete integral* K, see [5] and the expression (48) simplifies to

$$\sinh(z) = -\sinh\left(\frac{a}{4}\right)\mathrm{cn}(\widetilde{\alpha}t). \tag{49}$$

Finally, we obtain

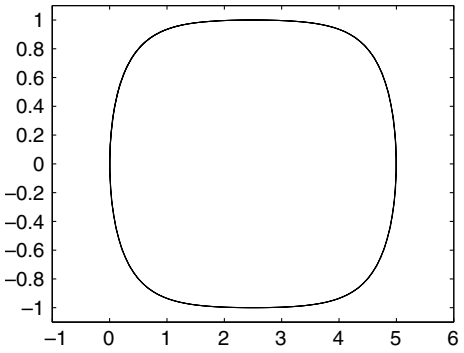

Fig. 7. Trajectory of one peakon.

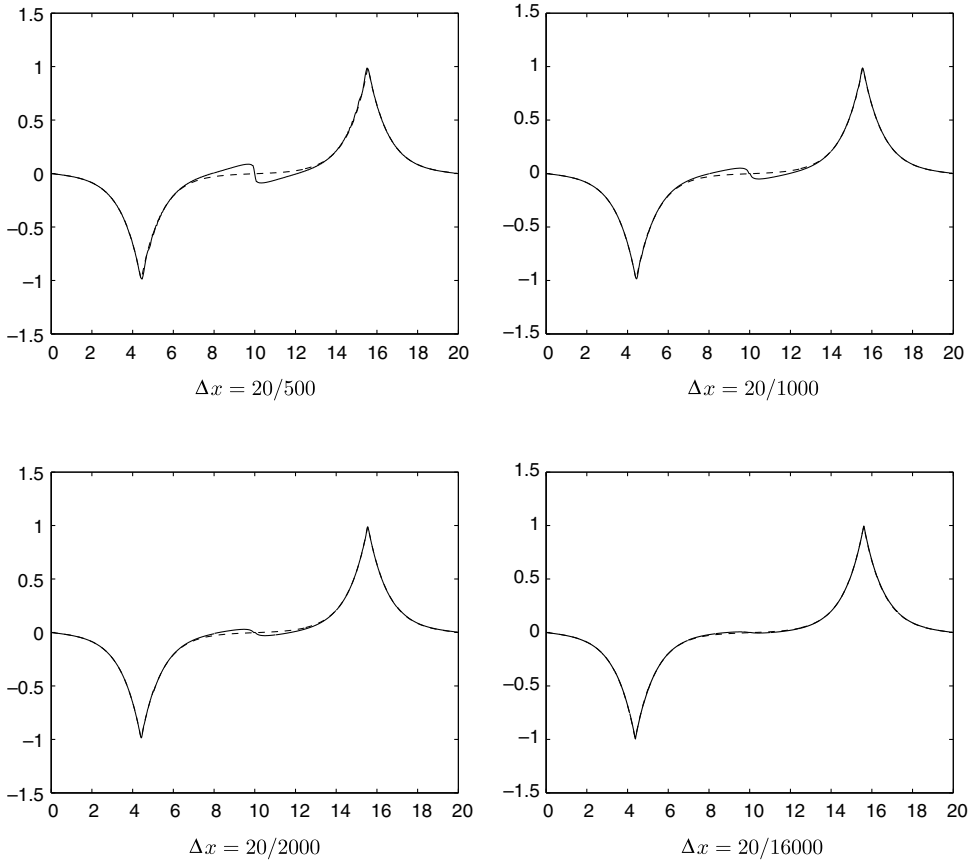

Fig. 8. Plot of the computed solution and the exact solution (in dash line) at time $t = 12$.

$$y = \frac{a}{4} - \sinh^{-1}\left(\sinh\left(\frac{a}{4}\right)\mathrm{cn}(\widetilde{\alpha}t)\right).$$

We can compute $u = y_t$, the height of the peak and get

$$u = \widetilde{\alpha}\tanh\left(\frac{a}{4}\right)\mathrm{sn}(\widetilde{\alpha}t).$$

In Fig. 7, we plot the trajectory of one peakon, that is, $(y(t), u(t))$.

From the position of the peaks (given by y) and their height (given by u), we reconstruct the solution $u(x,t)$ between the peaks as a linear combination of e^x and e^{-x}. The solution obtained this way will be considered as

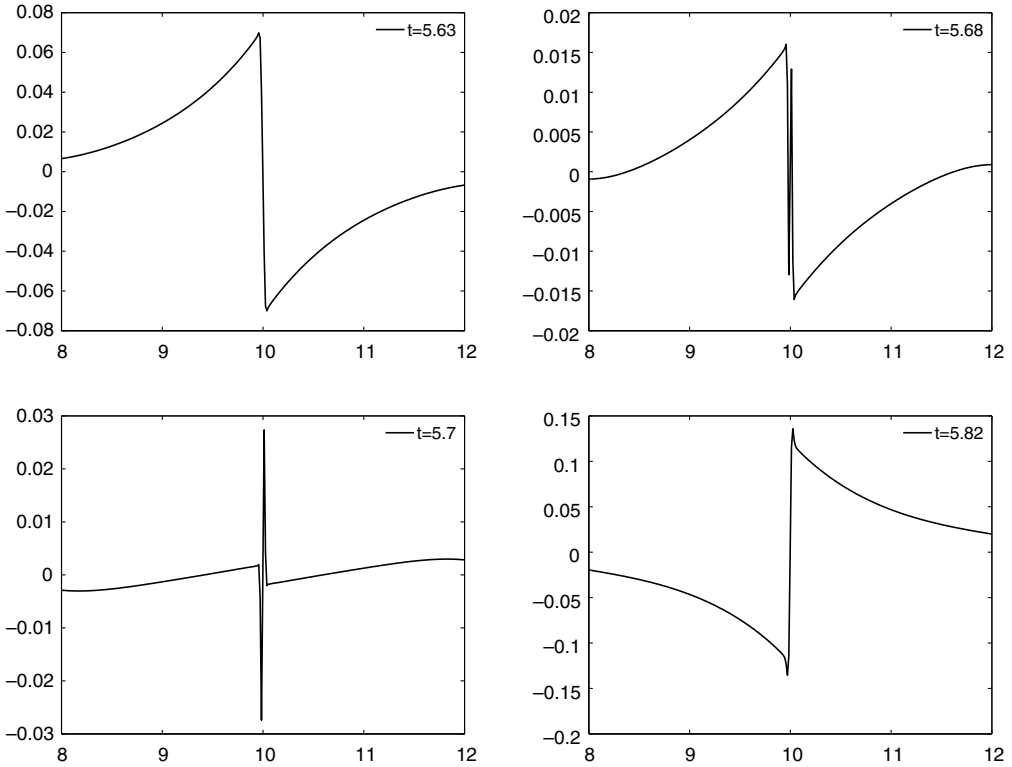

Fig. 9. Snapshots showing the collapse and resurrection of an antisymmetric peakon collision, $\Delta x = 0.0133$ and $\Delta t = 0.0024$.

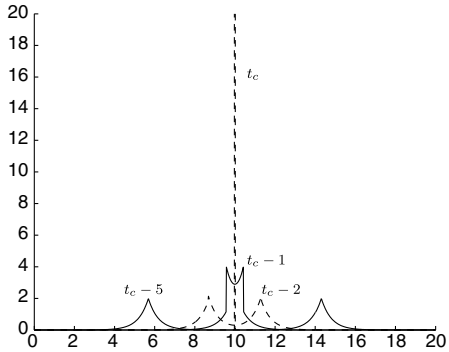

Fig. 10. Plot of the energy density, $(u^2 + u_x^2)(x,t)$, for the exact solution at different times before collision ($t_c \approx 5.69$ is the collision time).

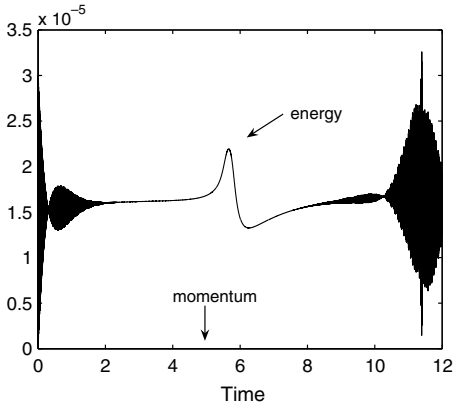

Fig. 11. Conservation of momentum (25) and energy (26) for the second multi-symplectic formulation, $\Delta x = 0.0133$ and $\Delta t = 0.0024$.

the reference solution. In the following numerical test, the initial values are set to $y(0) = a/4$ and $y_t(0) = u(0) = -1$. From (42), we have $E = 4\tanh^{-1}(\frac{a}{4})$.

We apply the multi-symplectic scheme (32) to the antisymmetric peakon collision with initial data from Fig. 1. The problem is integrated on the time interval [0, 12] and the spatial domain is [0, 20]. In Fig. 8, we can see that the scheme converges and that the main part of the error is concentrated around the point of collision, $x = 10$.

Fig. 9 shows the simulation in 4 snapshots taken just before and after that the collision takes place and we observe strong oscillations.

The difficulty to handle collisions can be explained by the low degree of regularity that the solution reaches when two peakons collide. Indeed, when the time t tends to the collision time, the energy density $(u^2 + u_x^2)(x,t)$ tends towards a Dirac, $E\sum_k \delta_{\frac{a}{2}+ka}(x)$ or $E\sum_k \delta_{ka}(x)$, see Fig. 10. Hence, the variable α, which stands for the energy density, has very low regularity as it becomes a Dirac function at collision time.

Finally, we plot the deviation of the momentum (25) and the energy (26) from their initial values, along the numerical solution of method (32). Note that in the evaluation of these integrals, we compute u_x^2 by means of α rather than using a finite difference approximation. Good conservation properties are observed for this scheme, even through the collision point (see Fig. 11).

4. Conclusion

With this paper, we have tried to see if the multi-symplectic philosophy could be useful for the Camassa–Holm equation. We have presented two new multi-symplectic formulations for this nonlinear partial differential equation. Basic linearly implicit multi-symplectic schemes were also derived, one allowing to describe peakon–antipeakon collisions.

So far, numerical tests have been conducted only with the Euler box scheme. It remains to try out and analyze implicit schemes like the Preissman box scheme or some multi-symplectic Runge-Kutta collocation methods. It would also be interesting to understand whether this formalism can be combined with the techniques found in the literature for approximating non-smooth solution, i.e., if multi-symplectic variants of such schemes can be found.

Since the multi-symplectic formulation of a partial differential equation is not unique, one can also try to find other such formulations of the Camassa–Holm equation and then derive other numerical schemes. Questions that immediately arise, are whether other multi-symplectic formulations will give different energy and momentum or not and if these quantities will be the next constants of motion in the series of Hamiltonian functions of the Camassa–Holm equation.

For all these reasons, it seems to us that it would be of interest to get more insight into the behaviour of multi-symplectic schemes for the Camassa–Holm equation.

Acknowledgments

We appreciate the referees' comments on an earlier version. We would like to thank Colin Cotter, Helge Holden, Robert McLachlan, and Sebastian Reich for interesting discussions. A part of this work was carried out when some of the authors visited the Isaac Newton Institute in Cambridge.

References

[1] Robert Artebrant, Hans Joachim Schroll, Numerical simulation of Camassa–Holm peakons by adaptive upwinding, Appl. Numer. Math. 56 (5) (2006) 695–711.
[2] Alberto Bressan, Adrian Constantin, Global conservative solutions of the Camassa–Holm equation, Arch. Ration. Mech. Anal. 183 (2) (2007) 215–239.
[3] Thomas J. Bridges, Multi-symplectic structures and wave propagation, Math. Proc. Cambridge Philos. Soc. 121 (1) (1997) 147–190.
[4] Thomas J. Bridges, Sebastian Reich, Multi-symplectic integrators: numerical schemes for Hamiltonian PDEs that conserve symplecticity, Phys. Lett. A 284 (4–5) (2001) 184–193.
[5] Paul F. Byrd, Morris D. Friedman, Handbook of elliptic integrals for engineers and scientists, Die Grundlehren der mathematischen Wissenschaften, Band 67, Second ed., Springer-Verlag, New York, 1971, revised.
[6] Roberto Camassa, Darryl D. Holm, An integrable shallow water equation with peaked solitons, Phys. Rev. Lett. 71 (11) (1993) 1661–1664.
[7] Roberto Camassa, Darryl D. Holm, James Hyman, A new integrable shallow water equation, Adv. Appl. Mech. 31 (1994) 1–33.
[8] Roberto Camassa, Jingfang Huang, Long Lee, On a completely integrable numerical scheme for a nonlinear shallow-water wave equation, J. Nonlinear Math. Phys. 12 (Suppl. 1) (2005) 146–162.
[9] Roberto Camassa, Jingfang Huang, Long Lee, Integral and integrable algorithms for a nonlinear shallow-water wave equation, J. Comput. Phys. 216 (2) (2006) 547–572.
[10] Giuseppe M. Coclite, Kenneth H. Karlsen, Nils H. Risebro, A convergent finite difference scheme for the Camassa–Holm equation with general H^1 initial data, SIAM J. NUMER. ANAL., in press.
[11] Adrian Constantin, On the scattering problem for the Camassa–Holm equation, R. Soc. Lond. Proc. Ser. A Math. Phys. Eng. Sci. 457 (2008) (2001) 953–970.
[12] Adrian Constantin, Joachim Escher, Global existence and blow-up for a shallow water equation, Ann. Scuola Norm. Sup. Pisa Cl. Sci. (4) 26 (2) (1998) 303–328.
[13] Adrian Constantin, Joachim Escher, Wave breaking for nonlinear nonlocal shallow water equations, Acta Math. 181 (2) (1998) 229–243.
[14] Adrian Constantin, Joachim Escher, Well-posedness, global existence, and blowup phenomena for a periodic quasi-linear hyperbolic equation, Comm. Pure Appl. Math. 51 (5) (1998) 475–504.
[15] Adrian Constantin, Boris Kolev, Least action principle for an integrable shallow water equation, J. Nonlinear Math. Phys. 8 (4) (2001) 471–474.
[16] Adrian Constantin, Boris Kolev, Geodesic flow on the diffeomorphism group of the circle, Comment. Math. Helv. 78 (4) (2003) 787–804.
[17] Adrian Constantin, Luc Molinet, Global weak solutions for a shallow water equation, Comm. Math. Phys. 211 (1) (2000) 45–61.
[18] Colin J. Cotter, Darryl D. Holm, Peter E. Hydon, Multisymplectic formulation of fluid dynamics using the inverse map, Preprint, 2007.
[19] Michael Fischer, Jeremy Schiff, The Camassa-Holm equation: conserved quantities and the initial value problem, Phys. Let. A 259 (5) (1999) 371–376.
[20] Benno Fuchssteiner, Some tricks from the symmetry-toolbox for nonlinear equations: generalizations of the Camassa–Holm equation, Phys. D 95 (3–4) (1996) 229–243.
[21] Benno Fuchssteiner, Athanassios S. Fokas, Symplectic structures, their Bäcklund transformations and hereditary symmetries, Phys. D 4 (1) (1981/82) 47–66.
[22] Helge Holden, Xavier Raynaud, Convergence of a finite difference scheme for the Camassa–Holm equation, SIAM J. Numer. Anal. 44 (4) (2006) 1655–1680 (Electronic).
[23] Helge Holden, Xavier Raynaud, A convergent numerical scheme for the Camassa–Holm equation based on multipeakons, Discrete Contin. Dyn. Syst. 14 (3) (2006) 505–523.
[24] Helge Holden, Xavier Raynaud, Global conservative solutions of the Camassa–Holm equation – a Lagrangian point of view, Comm. Partial Diff. Equat. 32 (10) (2006) 1511–1549.
[25] Helge Holden, Xavier Raynaud, Global conservative multipeakon solutions of the Camassa–Holm equation, J. Hyperbol. Differ. Equat. 4 (1) (2007) 39–63.
[26] Helge Holden, Xavier Raynaud, A numerical scheme based on multipeakons for conservative solutions of the Camassa–Holm equation, Hyperbolic Problems: Theory, Numerics, Applications, Springer, Berlin, 2008, pp. 873–881.
[27] Darryl D. Holm, J. Tilak Ratnanather, Alain Trouvé, Laurent Younes, Soliton dynamics in computational anatomy, Neuroimage 23 (2004) S170–S178.
[28] Robin S. Johnson, Camassa–Holm, Korteweg-de Vries and related models for water waves, J. Fluid Mech. 455 (2002) 63–82.

[29] Henrik Kalisch, Stability of solitary waves for a nonlinearly dispersive equation, Discr. Contin. Dyn. Syst. 10 (3) (2004) 709–717.
[30] Henrik Kalisch, Jonatan Lenells, Numerical study of traveling-wave solutions for the Camassa–Holm equation, Chaos Solit. Fract. 25 (2) (2005) 287–298.
[31] Shinar Kouranbaeva, Steve Shkoller, A variational approach to second-order multisymplectic field theory, J. Geom. Phys. 35 (4) (2000) 333–366.
[32] Yi. A. Li, Peter J. Olver, Convergence of solitary-wave solutions in a perturbed bi-Hamiltonian dynamical system. I. Compactons and peakons, Discr. Contin. Dynam. Syst. 3 (3) (1997) 419–432.
[33] Yi. A. Li, Peter J. Olver, Well-posedness and blow-up solutions for an integrable nonlinearly dispersive model wave equation, J. Differ. Equat. 162 (1) (2000) 27–63.
[34] Enrique Loubet, About the explicit characterization of Hamiltonians of the Camassa–Holm hierarchy, J. Nonlinear Math. Phys. 12 (1) (2005) 135–143.
[35] Jerrold E. Marsden, George W. Patrick, Steve Shkoller, Multisymplectic geometry, variational integrators, and nonlinear PDEs, Comm. Math. Phys. 199 (2) (1998) 351–395.
[36] Michael I. Miller, Alain Trouvé, Laurent Younes, On the metrics and Euler–Lagrange equations of computational anatomy, Ann. Rev. Biomed. Eng. 4 (2002) 375–405.
[37] Brian Moore, Sebastian Reich, Backward error analysis for multi-symplectic integration methods, Numer. Math. 95 (4) (2003) 625–652.
[38] Guillermo Rodríguez-Blanco, On the Cauchy problem for the Camassa–Holm equation, Nonlinear Anal. 46 (3, Ser. A: Theory Methods) (2001) 309–327.
[39] Yu-Shun Wang, Bin Wang, Xin Chen, Multisymplectic Euler box scheme for the KdV equation, Chin. Phys. Lett. 24 (2) (2007) 312–314.
[40] Yan Xu, Chi-Wang Shu, A local discontinuous Galerkin method for the Camassa–Holm equation, SIAM J. Numer. Anal., in press.